# Notch Ductile-to-Brittle Transition Due to Localized Inelastic Band

**Z. Suo**

**S. Ho**

**X. Gong**

Mechanical and Environmental Engineering Department,
University of California,
Santa Barbara, CA 93106-5070

*Holes are often drilled in a panel for cooling or fastening. For a panel made of a monolithic ceramic, such a hole concentrates stress, reducing load-carrying capacity of the panel by a factor of 3. By contrast, for a ductile alloy panel, plastic flow relieves stress concentration so that the small hole does not reduce load-carrying capacity. A panel made of ceramic-matrix composite behaves in the middle: matrix cracks permit unbroken fibers to slide against friction, leading to inelastic deformation which partially relieves stress concentration. Load-carrying capacity is studied in this paper as an outcome of the competition between stress concentration due to the notch, and stress relaxation due to inelastic deformation. The inelastic deformation is assumed to be localized as a planar band normal to the applied load, extending like a bridged crack. The basic model is large-scale bridging. A material length, $\delta_0 E/\sigma_0$, scales the size of the inelastic band, where $\sigma_0$ is the unnotched strength, $\delta_0$ the inelastic stretch at the onset of rupture, and E Young's modulus. Load-carrying capacity is shown to depend on notch size a, measured in units of $\delta_0 E/\sigma_0$. Calculations presented here define the regime of notch ductile-to-brittle transition, where ceramic-matrix composites with typical notch sizes would lie. Both sharp notches and circular holes are considered. The shape of the bridging law, as well as matrix toughness, is shown to be unimportant to load-carrying capacity.*

## 1 Introduction

Cottrell (1963) was among the first to recognize the full capacity of the work of Dugdale (1960), Barenblatt (1962), and Bilby et al. (1963), and put forth crack-bridging as a unifying process at all scales—from atomic debond to metal voiding. Instead of being viewed as a singularity, fracture, or any localized damage band, is now a gradual stretching of nonlinear springs. He also drew the analogy with the Peierls model, where a crystalline dislocation is a nonsingular, solitary solution of a spring-substrate system.

The crack-bridging concept integrates physical mechanisms of damage and macroscopic performance of materials in two steps. First, a sufficiently localized damage process is represented by nonlinear springs—be it electron cloud or metal ligament—with essential physical variables retained. Second, at a coarse scale, the interaction between the springs and the undamaged elastic substrate is viewed as a continuum problem. A common thread is that the spring law introduces a reference stress $\sigma_0$ and a reference length $\delta_0$, and that together with Young's modulus E of the substrate, they form a material length, $\delta_0 E/\sigma_0$, varying from a few nanometers for atomic decohesion, to a few centimeters for metal voiding. This material length determines the size of the inelastic deformation region. Cottrell was able to correlate notch-brittleness by the ratio of this material length to notch size.

Much has since been developed in vastly different contexts. A few recent examples are cited here. Metal-ceramic debonding is studied by Needleman (1990) on a basis of phenomenological spring laws mimicking atomic decohesion, and inelastic substrates representing background dislocation motion. Using springs with atomic periodicity, Rice (1992) reconsidered dislocation emission from a crack tip; instead of a full dislocation and a sharp crack (two singularities!), a dislocation now emerges incrementally from a crack tip, in a way analogous to Barenblatt's cleavage process. On a coarser scale, Huang and Hutchinson (1989) modeled shear localization by using springs representing void interaction. Suo (1991) examined domain band propagation in ferroelectric crystals under combined electric field and stress. Compressive kink band emanating from a hole is studied by Soutis et al. (1991) with springs representing fiber buckling. Using an earlier model of Aveston et al. (1971), Marshall et al. (1985) derived a bridging law representing frictional sliding, which set the basis for much of the subsequent work on composites.

Rice (1976) suggested two approaches to localization. In one approach, localization is due to loss of uniqueness, the entire band setting in simultaneously from a homogeneous field. In the second approach, a localization band nucleates at a material defect or a stress concentrator, spreading like a bridged crack. They are not equivalent, physically or mathematically. The second approach has the advantage that a physical length scale is introduced through bridging law, which links material performance with processing variables, such as fiber strength and fiber/matrix interface friction. The first approach seems to be irrelevant to ceramic-matrix composites, where the band con-

Contributed by the Materials Division and presented at the Symposium on Micromechanics of Ceramics and Ceramic Composites, Winter Annual Meeting, Anaheim, CA, November 8-13, 1992, of THE AMERICAN SOCIETY OF MECHANICAL ENGINEERS. Manuscript received by the Materials Division August 20, 1992; revised manuscript received November 1, 1992. Associate Technical Editor: S. Suresh.

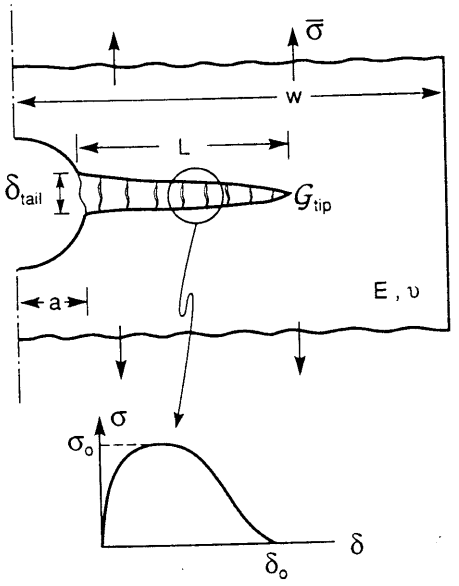


**Fig. 1 An inelastic band is viewed as either a bridged crack or an array of continuously distributed dislocations**

sisting of the matrix crack and sliding fibers nucleates from a processing flaw.

This paper is out of a more practical concern. We have been trying to reconcile design practices for ductile alloys and monolithic ceramics, and thereby provide a theoretical link between design *with* and design *of* ceramic-matrix composites. A representative design problem, notch sensitivity, is as follows. Holes are often drilled in a panel for fastening or cooling. In determining maximum load, a designer knows to ignore a small hole in a ductile metal panel, but not in a monolithic ceramic. What about a fiber-reinforced ceramic?

To focus the idea, Fig. 1 illustrates a panel with a hole, and the question is how much load the panel can carry. For a monolithic ceramic panel, the load should be such that the stress near the hole is below the strength of the ceramic. The latter is the Griffith stress associated with a cracklike flaw in the vicinity of the hole surface, of size close to grain diameter. Because of stress concentration, even a tiny hole reduces the load-carrying capacity by a factor of 3: ceramics are *notch-sensitive*. By contrast, a ductile alloy panel is designed with much tolerance. Plasticity relieves stress concentration, so that the maximum load should be such that the net-section fully yields. A small hole does not reduce the load-carrying capacity much: ductile alloys are notch-insensitive.

What about a fiber-reinforced ceramic? Without a hole, a composite sustains stress up to the fiber strength times the fiber volume fraction. The presence of a hole knocks down load-carrying capacity, but not necessarily by a factor of 3. Matrix cracks, allowing unbroken fibers to slide, partially relieve stress concentration. Elastic stress concentrates over a region that scales with the hole radius, $a$. On the other hand, sliding fibers provide extra deformation to redistribute stress over a region that scales with $\delta_0 E/\sigma_0$. Here $\delta_0$ is the extra displacement due to frictional sliding at the onset of fiber breaking, $\sigma_0$ the fiber strength times the fiber volume fraction, and E Young's modulus of the composite. Consequently, the ultimate load, $\bar{\sigma}_{max}$, is determined by the competition between elastic concentration and inelastic relaxation:

$$\frac{a}{\delta_0 E/\sigma_0} = \begin{cases} 0, \text{ notch—ductile, } \bar{\sigma}_{max}/\sigma_0 = 1 \\ \infty, \text{ notch—brittle, } \bar{\sigma}_{max}/\sigma_0 = 1/3. \end{cases} \quad (1)$$

Both material and notch size are important: for a given composite, a large hole reduces load-carrying capacity by a factor close to 3, but a small hole does not reduce it as much. Large or small, hole radius $a$ is measured in units of material length $\delta_0 E/\sigma_0$.

This concept places design practices into perspective. Take $a = 1 \sim 10$ mm in usual engineering practice and take, for ceramic-matrix composites, $\delta_0 E/\sigma_0 = 0.1 \sim 10$ mm. As our calculation will show, these put a notched composite into the ductile-to-brittle transition regime. Criterion (1) also prompts the notion of designing materials for a given application. For ceramic-matrix composites, the limiting-separation $\delta_0$ can be varied, by orders of magnitude, by varying fiber radius, fiber strength and fiber-matrix interface friction. Thus, a composite may be *engineered* to make a hole ductile for a required hole size.

In a broader context, $\delta_0 E/\sigma_0$ serves as a figure of merit of ductility. The ultimate strain of an unnotched bar in tension is not a good measure of ductility; it depends on gauge length and the number of deformation bands. Cross-section reduction is a valid measure of ductility for metals, but is not transferable to a notched component, nor does it have any counterpart in composites.

The basic ideas outlined above and a few preliminary results have been discussed in a review article by Bao and Suo (1992). The present paper is to supply mechanics calculations that define the ductile-to-brittle transition regime, where ceramic-matrix composites—with holes of useful sizes—would lie. A more general theme pursued here, as well as in the previous article, is to search for commonality in large-scale bridging models, where Irwin's linear fracture mechanics breaks down. A dilemma which has become evident over the last few years is this. While crack-bridging concepts are versatile to explain many phenomena, the mechanics analyses—and interpretations—are complicated enough to be author-dependent, particularly in the large-scale bridging regime. At this stage, any simplification or integration would help.

## 2 The Model

**2.1 Dimensionless Groups.** Figure 1 defines the general mechanics problem: a band of inelastic deformation emanates from a notch in a component monotonically loaded by $\bar{\sigma}$. The band is *localized* in that its thickness is much smaller than any other lengths characterizing the component. The load $\bar{\sigma}$ can be regarded as a function of the stretch at the band-tail, $\delta_{tail}$; the band length $L$ is an internal variable to be determined by the model. The model will predict the ultimate stress, or *load-carrying capacity*, $\bar{\sigma}_{max}$, of the notched component. The answer takes the functional form

$$\bar{\sigma}_{max}/\sigma_0 = \mathcal{F}(\alpha, \gamma). \quad (2)$$

Also entering the right-hand side are the bridging law shape, and the ratios of $\alpha$ to other lengths of geometry, such as notch root radius and panel width. The rest of this subsection explains these dimensionless groups.

The inelasticity may be divided into that localized in the band, and that further localized at the band tip. The inelasticity in the band is modeled as an array of springs with a nonlinear stress-stretch relation:

$$\sigma/\sigma_0 = \chi(\delta/\delta_0). \quad (3)$$

The dimensionless function $\chi$ describes the shape of the relation; the scale is set by a reference stress, $\sigma_0$, and a reference stretch, $\delta_0$. Figure 2 shows several bridging laws to be used in numerical calculations. The second mechanism is represented by a critical energy release rate at the tip, $\Gamma_0$. For a ceramic-matrix composite with debonded fibers, the inelastic stretch is due to sliding between fibers and matrix, and $\Gamma_0 = (1-f)\Gamma_m$, where $f$ is fiber volume fraction and $\Gamma_m$ matrix fracture energy. For a void band in a ductile alloy, the band stretches at the

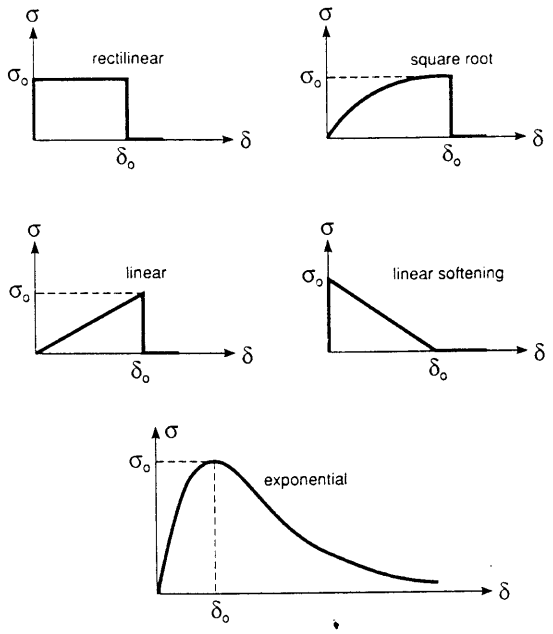


**Fig. 2 Idealized bridging laws**

expense of enlarging voids, and $\Gamma_0$ dissipates in creating new voids by inclusion/matrix debonding.

The relative magnitude of the two inelastic mechanisms is described by the dimensionless number

$$\gamma = \Gamma_0/\sigma_0\delta_0. \tag{4}$$

It enters (2) to determine load-carrying capacity. Two limiting cases are of particular significance. When $\gamma \to \infty$, the energy dissipation in the band is insignificant compared to that at the tip, so that Linear Fracture Mechanics applies. However, for composites and ductile alloys, inelastic dissipation of the band dominates, say $\gamma < 0.1$. This paper focuses on the latter case.

Outside the band, the material is taken to be isotropic and linearly elastic, E being Young's modulus, $\nu$ Poisson's ratio, and $E' = E$ for plane stress and $E' = E/(1-\nu^2)$ for plane strain. The coupled substrate-spring defines a material length

$$\delta_0 E'/\sigma_0. \tag{5}$$

This length serves as a figure of merit for the ductility of a bridging mechanism. The dimensionless group

$$\alpha = \frac{a}{(\delta_0 E'/\sigma_0)} \tag{6}$$

measures the size of the notch, $a$, in units of the material length. Observe that $\alpha$ enters (2) as a *size effect*.

**2.2 Mathematic Description.** The basic model is large-scale bridging; see Bao and Suo (1992) for references. An inelastic band can be viewed as either a bridged crack, or an array of continuously distributed dislocations. An inelastic band and a traction-free crack behave the same at their tips. The stress a short distance $r$ ahead of the band-tip is square root singular:

$$\sigma_y = K_{tip}(2\pi r)^{-1/2}, \quad r/L \to 0. \tag{7}$$

Here $K_{tip}$ is Irwin's stress intensity factor. The stretch a short distance $r$ behind the band-tip is parabolic:

$$\delta = 8(K_{tip}/E')(r/2\pi)^{1/2}, \quad r/L \to 0. \tag{8}$$

This may be verified by superimposing the result for a pair of concentrated force, on crack faces that are otherwise free of traction. Irwin's relation connects the stress intensity factor and the energy release rate at the band-tip:

$$\mathcal{G}_{tip} = K_{tip}^2/E'. \tag{9}$$

We will use $\mathcal{G}_{tip}$ and $K_{tip}$ interchangeably.

An inelastic band is also equivalent to an array of continuously distributed dislocations (e.g., Cottrell, 1963). The stress in the spring, at position $x$, is due both to the applied stress $\bar{\sigma}$, and to the dislocation array:

$$\sigma_0\chi(\delta/\delta_0) = \bar{\sigma}F(x/a) + \frac{E'}{a}\int_a^{a+L} H(x/a, \xi/a)\frac{\partial\delta}{\partial\xi}\,d\xi. \tag{10}$$

Here $F$ and $H$ are known functions; this integral equation governs the stretch $\delta(x)$, which can be solved numerically (Gu et al., 1992).

Of direct bearing on load-carrying capacity are the tail-stretch $\delta_{tail}$, and the band-tip energy release rate $\mathcal{G}_{tip}$ (Fig. 1). Normalizing (10) by

$$\bar{\sigma}/\sigma_0,\ \delta/\delta_0,\ x/a,\ \xi/a,\ L/a, \tag{11}$$

one finds that the answers take the forms

$$\bar{\sigma}/\sigma_0 = f(\delta_{tail}/\delta_0,\ \alpha,\ L/a), \tag{12}$$

and

$$\mathcal{G}_{tip}/\sigma_0\delta_0 = g(\delta_{tail}/\delta_0,\ \alpha,\ L/a). \tag{13}$$

The functions $f$ and $g$ will also depend on the bridging law shape $\chi$ and the ratios of $a$ to other lengths of geometry, but nothing else. Note that $\mathcal{G}_{tip}$ may be obtained from $\delta(x)$ according to (8) and (9).

For hardening bridging, at fixed $\alpha$ and $L/a$, $\bar{\sigma}$ monotonically increases with $\delta_{tail}$, so that either one can be prescribed in solving (10). This is not so for softening bridging; $\bar{\sigma}$ may first increase with $\delta_{tail}$, reaching a peak, and then drop. Thus, in general, $\delta_{tail}$ should be prescribed in a calculation. Given a notched component, $\alpha$ and $\gamma$ are fixed; upon loading, the applied stress $\bar{\sigma}$ is a function of tail-stretch $\delta_{tail}$. The band length $L$, being regarded as an internal variable, is to be determined from (13) by maintaining $\mathcal{G}_{tip} = \Gamma_0$. Load-carrying capacity $\bar{\sigma}_{max}/\sigma_0$ is the maximum as $\delta_{tail}$ varies within the range allowed by the bridging law. We therefore confirm (2).

**2.3 A Simplification.** For well-toughened materials, band-tip dissipation is negligible, $\gamma = \Gamma_0/\sigma_0\delta_0 \ll 1$. A drastic simplification is suggested by *steady-state banding*. When the band is long compared to the notch size, $\mathcal{G}_{tip}$ becomes independent of $L/a$ and notch shape, being equal to the complementary energy of the spring law (Budiansky et al., 1986; Rose, 1987). For example,

$$\mathcal{G}_{tip}^{ss} = \frac{1}{3}\sigma_0\delta_0(\bar{\sigma}/\sigma_0)^3 \tag{14}$$

for the square-root law $\chi(\epsilon) = \sqrt{\epsilon}$. Consequently, if $\gamma = \Gamma_0/\sigma_0\delta_0$ is small, the band runs across the entire component at a low load $\bar{\sigma}/\sigma_0$, leaving springs intact.

The cross-component band is nonuniformly stretched, $\delta_{tail} > \bar{\delta}$, where $\bar{\delta}$ is related to $\bar{\sigma}$ by the spring law. The dimensional argument similar to that leading to (12) now gives

$$\bar{\sigma}/\sigma_0 = S(\delta_{tail}/\delta_0, \alpha). \tag{15}$$

Obviously, no equation analogous to (13) exists in this case. The maximum $\bar{\sigma}_{max}$ can thus be determined as $\delta_{tail}$ varies within the range allowed by the bridging law. The rest of the article will focus on presenting results for the special case $\gamma = 0$, with occasional excursion to the case of small $\gamma$, only to show the insignificance of the latter as far as load-carrying capacity is concerned.

Figure 2 shows bridging laws representative of a wide range of behaviors; their solutions are summarized in the Appendix. A few simple observations are made here. Rectilinear and linear-softening laws cause a peculiarity; they have no complementary energy, $\mathcal{G}_{tip}^{ss} = 0$. Thus, the band length $L$ is finite even if $\gamma = 0$, and should be determined from (13).

The exponential law

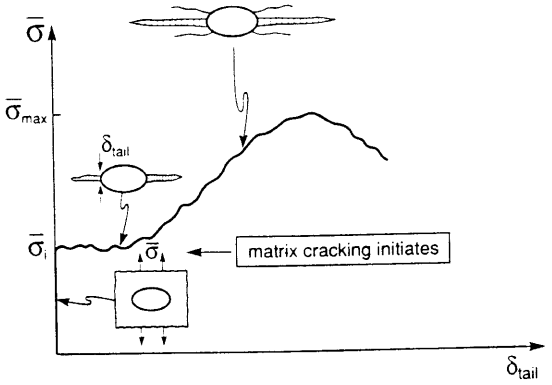


**Fig. 3 Damage progression in ceramic-matrix composites**

$$\sigma/\sigma_0 = (\delta/\delta_0)\exp(1-\delta/\delta_0) \tag{16}$$

is taken by Needleman (1990) to represent atomic decohesion. The two reference quantities, $\sigma_0$ and $\delta_0$, can be inferred in the usual way from measurable cohesive properties—lattice spacing, Young's modulus and surface energy. This law is used here to illustrate all laws of this type. First, the law has no limiting-stretch; $\delta_0$ is assigned, arbitrarily, as the stretch where the stress reaches the maximum, $\sigma_0$. Nonetheless, $\delta_0$ still conveys the idea of interaction range ($\delta_0 \sim 1$ Å for atomic debond). Second, due to softening in the springs, for fixed $\alpha$ in (15), $\bar{\sigma}$ first increases with $\delta_{tail}$, reaching a maximum, and then drops. Third, uniqueness is not guaranteed for systems with softening. In fact, for the defect-free case ($\alpha = 0$), multiple solutions are found, ranging from periodic to solitary (Suo et al., 1992b). However, uniqueness seems to prevail when a defect is present.

## 3 Damage Progression in Ceramic Composites

To be definite, the model is now interpreted in the context of ceramic-matrix composites, even though conclusions may be applicable to other inelastic mechanisms. Figure 3 is a schematic of damage progression in a notched component under monotonic loading $\bar{\sigma}$. A matrix crack initiates at $\bar{\sigma} = \bar{\sigma}_i$; prior to this, $\delta_{tail} = 0$. For a crack-like notch, $\bar{\sigma}_i$ is governed by notch size $a$, according to Griffith's formula

$$\bar{\sigma} = (E'\Gamma_0/\pi a)^{1/2}. \tag{17}$$

This stress is insensitive to processing flaws in the matrix, so long as the flaws are much smaller than the notch size.

For a circular hole, an initial flaw must be assumed in the vicinity of the hole, of size, say, on the order of the fiber diameter. Take the flaw to be a traction-free, penny-shaped crack of diameter, $d$, so that

$$\bar{\sigma}_i = \frac{1}{3}(\pi E'\Gamma_0/2d)^{1/2}. \tag{18}$$

This has been reduced by the stress concentration factor 3, and assumes that the fibers and matrix have similar elastic constants. In practice $\bar{\sigma}_i$ may also depend on the hole radius $a$, for a larger hole concentrates stress in a wider region, increasing the chance to trigger a bigger defect. Since $a \gg d$, the cracking initiation stress is larger for a hole than for a crack-like notch. In either case further loading may be sustained without fiber breaking. Consequently, $\bar{\sigma}_i$ is unimportant as far as the ultimate strength is concerned.

After extending into the component, the crack is bridged by the fibers sliding against friction. This inelastic deformation can be represented by a bridging law (Marshall et al., 1985)

$$\sigma/\sigma_0 = (\delta/\delta_0)^{1/2} \tag{19}$$

Upon assuming a deterministic fiber strength $S$, one has

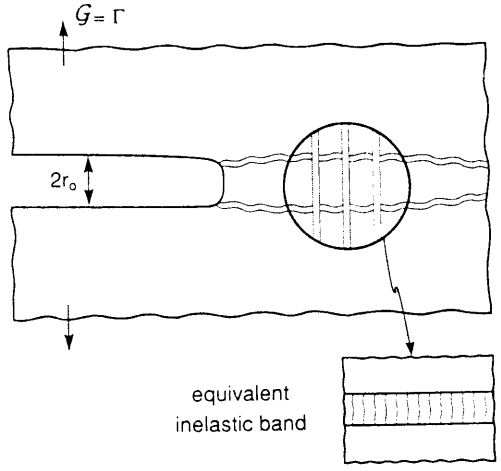


**Fig. 4 Multiple cracks modeled as an inelastic band**

$$\sigma_0 = fS, \tag{20}$$

and

$$\delta_0 = \frac{R}{2}\left(\frac{E_m}{E}\right)^2 \frac{(1-f)^2 S^2}{\tau E_f}. \tag{21}$$

Here $f$ is the fiber volume fraction, $R$ the fiber radius, $\tau$ the sliding friction of fiber/matrix interface, and E, $E_m$, and $E_f$ are Young's moduli for the composite, matrix and fiber, respectively. In terms of primary processing variables, the material length identified in Section 2 now scales as

$$\delta_0 E/\sigma_0 \propto RS/\tau. \tag{22}$$

Thus, the "ductility" of a composite increases with increasing fiber radius and fiber strength, but decreases with increasing friction of the fiber-matrix interface.

In practice, the fiber strength is statistical; $S$ is taken to be some average value, since the ultimate stress of a composite corresponds to the breaking of many fibers. It is wrong to take $\delta$ as physical separation of the matrix crack. As pointed out by Hutchinson and Jensen (1990), $\delta$ should be inelastic deformation associated with frictional sliding—that is, total elongation of the composite with a matrix crack minus the elastic deformation of the composite without the matrix crack. The inelastic band consists of both the matrix crack and the frictional dissipation off the crack plane. The above equations were derived from an approximate analysis of fibers frictionally constrained in a matrix, and are valid when the slip length

$$l = \frac{R}{2}\frac{E_m(1-f)}{Ef}\frac{\sigma}{\tau} \tag{23}$$

is several times fiber radius, which is typically the case in ceramic-matrix composites. Also note that the square-root law is only valid prior to fiber breaking. Yet design with ceramic-matrix composites may allow matrix cracking to relieve stress concentration, but require fibers to remain unbroken, so that the square-root law is adequate for this purpose.

An important feature is multiple cracks. Broadly, multiple cracks provide additional frictional dissipation sites or, equivalently, larger inelastic deformation to relieve stress concentration. As an illustration, consider multiple cracks emanating from a long, blunt notch in Fig. 4. The matrix is assumed to be sufficiently brittle so that these cracks run across the component at a low load without fibers breaking. If the slip lengths do not overlap with one another and each spring is described by (19), the fracture energy is given by

$$\Gamma = \frac{2}{3}\sigma_0\delta_0\mathfrak{N}, \tag{24}$$

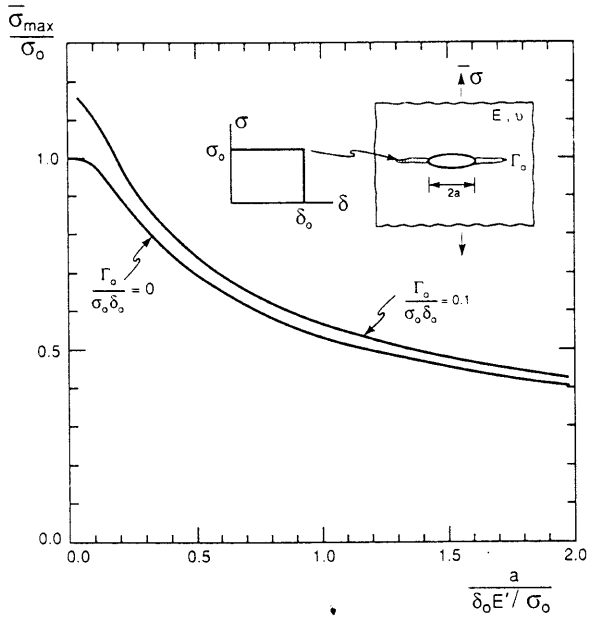


Fig. 5 Effect of the two primary dimensionless groups

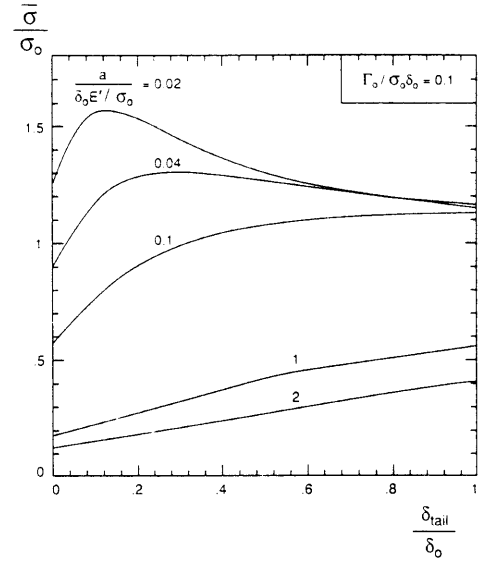


Fig. 6 Relation between load and tail-separation (rectilinear bridging)

where $\mathfrak{N}$ is the number of cracks, presumably related to the ratio of notch root radius over slip length. More detailed modeling is needed to take into account overlapping slip, analogous to models for unnotched panels by Aveston et al. (1971) and Zok and Spearing (1992). Nonetheless, to a first approximation, the effect of multiple cracks on load-carrying capacity may be captured by a single inelastic band with a larger equivalent $\delta_0$.

## 4 Notch Size and Matrix Toughness: $\alpha$ and $\gamma$

Now the calculated load-carrying capacity is presented in form (2). The strength of a monolithic ceramic is only a fraction of its bridging strength (the atomic bond), and is sensitive to processing flaws. By contrast, the strength of a composite is close to its bridging strength (the fiber strength times fiber volume fraction), and is insensitive to processing flaws. To understand this difference, consider an unbridged crack of length $2a$, as in Fig. 5. The inelasticity—either atomic separation or fiber sliding—is approximated by a rectilinear law in the band, and by $\Gamma_0 = 0$ at the band tip. The standard solution is reproduced in the Appendix. Under monotonic loading $\bar{\sigma}$, the band length $L$ is determined from (A4) by maintaining $K_{tip} = 0$. The ultimate stress $\bar{\sigma}_{max}$ is reached when $\delta_{tail} = \delta_0$. Eliminating the internal variable $L$ from (A3) and (A4), Cottrell (1963) obtained that

$$\frac{8}{\pi}\left(\frac{a}{\delta_0 E'/\sigma_0}\right)\ln\left[\sec\left(\frac{\pi}{2}\frac{\bar{\sigma}_{max}}{\sigma_0}\right)\right] = 1. \tag{25}$$

This curve is labeled in Fig. 5 by $\Gamma_0/\sigma_0\delta_0 = 0$, to show load-carrying capacity as a function of notch size.

For a fine grain ceramic, energy dissipates to separate a few atoms at the crack tip, so that $\delta_0 E'/\sigma_0 \sim 1$ nm; the flaw size is about the grain diameter, say $a \sim 1$ μm. Consequently, $\alpha \sim 10^3$ so that $\bar{\sigma}_{max}/\sigma_0 \ll 1$, confirming that the strength of a monolithic ceramic is much smaller than that of the atomic bond. By contrast, for a ceramic-matrix composite, energy dissipates over many atoms by interface sliding, say $\delta_0 E'/\sigma_0 \sim 1$ mm; material processing is unlikely to break many fibers on the same location, so that $\alpha < 1$. Consequently, the strength is close to the limiting stress $\bar{\sigma}_{max} \sim \sigma_0 = fS$, and is insensitive to processing defects. This comparison reveals the central concept of making strong materials: the limiting-strength for a composite is very low compared with atomic bond strength, but amply compensated by a large inelastic stretch $\delta_0$, which retains this strength in the presence of flaws or small notches.

Next consider the case $\Gamma_0/\sigma_0\delta_0 = 0.1$, which is perhaps the largest value any well-toughened ceramic-matrix composite may assume. The left-hand side of (A3) equals $\delta_{tail}/\delta_0\alpha$, and the left-hand side of (A4) equals $(\gamma/\pi\alpha)^{1/2}$. Thus, for fixed $\alpha$ and $\gamma$, (A3) and (A4) prescribe the applied stress $\bar{\sigma}/\sigma_0$ as a function of $\delta_{tail}/\delta_0$, the band length $L/a$ being viewed as an internal variable. This $\bar{\sigma} - \delta_{tail}$ relation is plotted in Fig. 6 for $\gamma = 0.1$ and various $\alpha$. Depending on $\alpha$, the maximum $\bar{\sigma}_{max}/\sigma_0$, is reached at either $\delta_{tail}/\delta_0 = 1$ or $\delta_{tail}/\delta_0 < 1$. The maxima so obtained are plotted in Fig. 5. Except for very small $\alpha$, the difference between the two curves is small. The curve for $\gamma = 0.1$ tends to infinity for small, $\alpha$, which is consistent with Griffith theory. However, this difference is practically inconsequential, for it only happens for a notch smaller than fiber diameter. Corresponding plots have been made for the linear bridging law and for a circular hole (not shown here); the trend is similar to Fig. 5. In the rest of the paper, we shall focus on the case $\Gamma_0/\sigma_0\delta_0 = 0$.

## 5 Bridging Law Shape

The shape of the bridging law is uncertain in practice. Fortunately, load-carrying capacity is a robust quantity: a different $\chi$ only modifies it slightly, not to affect the judgement of a designer (e.g., notch-brittle or -ductile). Figure 7 demonstrates this for a sharp notch in an infinite panel, and Fig. 8 for a circular hole. On the basis of the preceding discussion, it is sufficient to consider the case $\Gamma_0/\sigma_0\delta_0 = 0$, so that the inelastic band has extended across the component for bridging laws with nonvanishing complementary energy. The curves in Figs. 7 and 8 may shift somewhat as more accurate calculations become available, but the small difference in load-carrying capacity for the various bridging laws may be inconsequential in practice. An explanation for such small differences follows.

Instead of $\alpha$, a modified dimensionless group, $a/(E'\Gamma/\sigma_0^2)$, is used in Fig. 7, where $\Gamma$ is the energy to separate a unit area of the inelastic band:

$$\Gamma = \sigma_0\delta_0\int_0^\infty \chi(\epsilon)d\epsilon. \tag{26}$$

As discussed in Section 3, the inelastic band may consist of

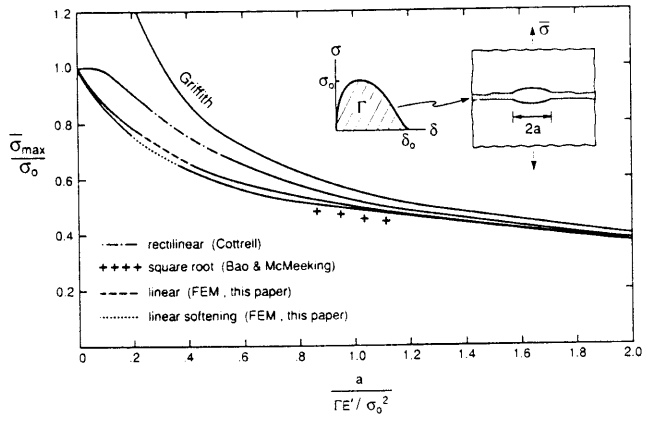


Fig. 7 Notch ductile-to-brittle transition (sharp notch)

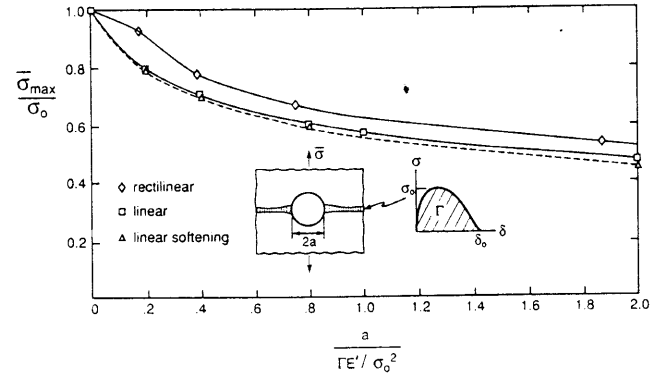


Fig. 8 Notch ductile-to-brittle transition (circular hole)

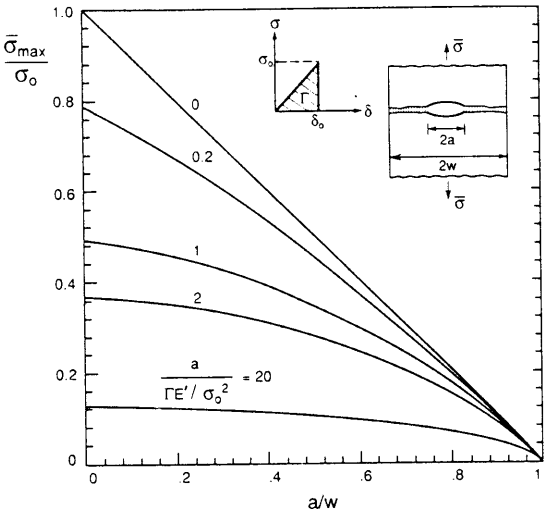


Fig. 9 Effect of *a/w* (sharp notch)

several matrix cracks, each permitting fibers to slide, so that $\delta_0$ should be regarded as the sum of all inelastic deformation.

Two limiting cases can be solved analytically; both are independent of bridging law shape. As $\alpha \to 0$, stress concentration is fully relieved—that is, $\bar{\sigma}_{max}/\sigma_0 = 1$. As $\alpha \to \infty$, the unbridged crack is long so that Griffith's formula applies:

$$\bar{\sigma}_{max}/\sigma_0 = [\pi a/(E'\Gamma/\sigma_0^2)]^{-1/2}. \quad (27)$$

This curve is indicated in Fig. 7, which is only valid for large $\alpha$. The mechanics problem involved here, which consists of two elastic substrates joined by springs (inset of Fig. 7), is different from that in Griffith's original paper. Nonetheless (27) can be confirmed by an energy argument. A simple interpolation of the two limiting cases is

$$\bar{\sigma}_{max}/\sigma_0 = [1 + \pi a/(\Gamma E'/\sigma_0^2)]^{-1/2}. \quad (28)$$

This is a close approximation of the computed result for the liner law, and a fair representation of the curves for other laws. One can use this equation for arbitrary $\alpha$, as an extrapolation of the Griffith formula (27).

Equation (28) can also be derived from an energy consideration. Under the applied load $\bar{\sigma}$, the springs are nonuniformly stretched: $\delta_{tail} > \bar{\delta}$, where $\bar{\delta}$ and $\bar{\sigma}$ are related by the spring law. In equilibrium, the increment of the combined strain energy in the substrates and springs must vanish for any small increment of the notch size. Thus,

$$\sigma_0\delta_0 \int_{\bar{\delta}/\delta_0}^{\delta_{tail}/\delta_0} \chi(\epsilon)d\epsilon \approx \pi a\bar{\sigma}^2/E'. \quad (29)$$

The left-hand side is the energy decrease in the springs, and the right-hand side the energy increase in the substrates, for a unit enlargement of the notch under fixed load. The latter is approximate, with relaxation due to the springs ignored. Equation (29) becomes exact as $\alpha \to \infty$, which reduces to (27); and is also correct as $\alpha \to 0$, since $\delta_{tail} = \bar{\delta}$ in this case. Specializing (29) for the linear law $\chi(\epsilon) = \epsilon$, one obtains (28).

Plotted in Fig. 8 is the load-carrying capacity reduced by a circular hole, which is constructed by using finite element solutions, discussed in the Appendix. Note that the difference for various bridging laws is still small, and that the two limiting cases are given by (1).

Normalized as such, it appears from Figs. 7 and 8, that load-carrying capacity is insensitive to bridging law shape. We have not carried out comparisons other than for notches in an infinite panel. Nonetheless the normalization scheme used here separates the roles of the *shape* and the *scale* of a bridging law. This is of practical significance. Once charts are constructed for idealized bridging laws with important design features (e.g., fasteners), a new material can be used by fitting its bridging law to one of the idealized laws. This approach is equally valuable in design of composites. In this phase, the detailed bridging law shape may be unknown, but the scale of the bridging, $\sigma_0$ and $\delta_0$, can be related to microstructural variables. Whether a material is viable for a particular application can be assessed, before the material is made, by consulting the charts.

## 6 Effect of *a/w*

The effect of finite panel width is studied with $\Gamma_0/\sigma_0\delta_0 = 0$. The model consists of halves joined by springs, with an unbridged sharp notch (Fig. 9) and a circular hole (Fig. 10). Independent of bridging law, full notch-ductility is reached when $a/(\Gamma E'/\sigma_0^2) = 0$. Stress concentration is completely relieved, so the load-carrying capacity is governed by the net-section:

$$\bar{\sigma}_{max}/\sigma_0 = 1 - a/w. \quad (30)$$

This is the straight line in Figs. 9 and 10.

Notch-brittleness prevails for large $a/(\Gamma E'/\sigma_0^2)$. In this limit, Linear Elastic Fracture Mechanics applies for a sharp notch, regardless of the bridging law shape. Thus,

$$\frac{\bar{\sigma}_{max}}{\sigma_0} = \left[\pi F^2 \frac{a}{\Gamma E'/\sigma_0^2}\right]^{-1/2}, \quad (31)$$

where $F$ is a dimensionless number in the stress intensity factor for a crack in an elastic strip, approximated by (Tada et al., 1985)

$$F(a/w) = [1 - 0.5(a/w) + 0.326(a/w)^2][1 - (a/w)]^{-1/2}. \quad (32)$$

An interpolation similar to (28) is

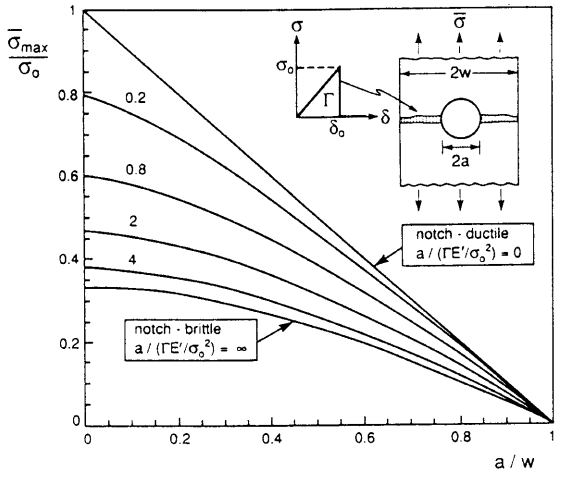


**Fig. 10 Effect of *a/w* (circular hole)**

$$\frac{\bar{\sigma}_{max}}{\sigma_0} = \left[ \left(1 - \frac{a}{w}\right)^{-2} + \pi F^2 \frac{a}{\Gamma E'/\sigma_0^2} \right]^{-1/2}. \quad (33)$$

This equation is plotted in Fig. 9, and expected to be a fair approximation for the entire parameter range and arbitrary bridging law, and highly accurate when $a/(\Gamma E'/\sigma_0^2) > 2$, as inferred from Fig. 7.

For a circular hole, when $a/(\Gamma E'/\sigma_0^2)$ is large, load-carrying capacity is reduced by the stress concentration factor $k$, namely

$$\bar{\sigma}_{max}/\sigma_0 = 1/k. \quad (34)$$

The handbook solution (e.g., Peterson, 1974) of the stress concentration factor for a circular hole in an elastic strip, $k$, is indicated in Fig. 10, as the boundary of notch-brittleness. A finite element calculation using linear springs is carried out for intermediate $a/(\Gamma E'/\sigma_0^2)$. Linearity suggests that the stress at the band-tail takes the form

$$\sigma_{tail} = \bar{\sigma} f(\alpha, a/w). \quad (35)$$

The applied load $\bar{\sigma} \to \bar{\sigma}_{max}$ when $\sigma_{tail} = \sigma_0$, so that $\bar{\sigma}_{max}/\sigma_0 = 1/f$. The calculated coefficient $f$ is plotted in Fig. 10. Judged from Fig. 8, the curves in Fig. 10 should be fair approximations for other bridging laws.

## 7 Concluding Remarks

Notch-sensitivity can be substantially reduced by inelastic deformation. In a ceramic-matrix composite, the inelastic deformation is due to one or several matrix cracks bridged by frictionally sliding fibers. The strength of notched ceramic-matrix composites is found to depend on notch size, as governed by a dimensionless group $a/(\delta_0 E'/\sigma_0)$. Notch-insensitivity is attained if the composite is made such that $a/(\delta_0 E'/\sigma_0) \leq 1$. It is found that the shape of the bridging law is unimportant as far as notch strength is concerned. Although the results are interpreted for ceramic-matrix composites, they may be applicable for other materials or inelastic mechanisms. For example, the notch strength presented here is the same as the residual strength of a metal-matrix composite with a fatigue-cracked matrix.


### Acknowledgment

We are grateful to Professor B. Budiansky for a stimulating conversation, and to Professors A. G. Evans, F. A. Leckie, and F. W. Zok for inspiration. Financial support is provided by ONR/URI contract N00014-92-J-1808. Finite element analyses are carried out using ABAQUS.


### References


Aveston, J., Cooper, G. A., and Kelly, A., 1971, "Single and Multiple Fracture," *The Properties of Fiber Composites*, IPC Science and Technology Press, UK.

Bao, G., and McMeeking, R. M., 1992, "Fatigue Crack Growth in Fiber-Reinforced Metal-Matrix Composites," *J. Mech. Phys. Solids.*, in press.

Bao, G., and Suo, Z., 1992, "Remarks of Crack-Bridging Concepts," *Appl. Mech. Rev.*, Vol. 24, pp. 355-366.

Barenblatt, G. I., 1962, "The Mathematical Theory of Equilibrium Cracks in Brittle Fracture," *Adv. Appl. Mech.*, Vol. 7, pp. 55-129.

Bilby, B. A., Cottrell, A. H., and Swinden, K. H., 1963, "The Spread of Plastic Yielding from a Notch," *Proc. Roy. Soc. Lond.*, Vol. A272, pp. 304-314.

Budiansky, B., Hutchinson, J. W., and Evans, A. G., 1986, "Matrix Fracture in Fiber-Reinforced Ceramics," *J. Mech. Phys. Solids*, Vol. 34, pp. 167-189.

Cottrell, A. H., 1963, "Mechanics of Fracture," *Tewksbury Symposium of Fracture*, University of Melbourne, Australia, pp. 1-27.

Cui, L., and Budiansky, B., 1992, private communication.

Dugdale, D. S., 1960, "Yielding of Steel Sheets Containing Slits," *J. Mech. Phys. Solids*, Vol. 8, pp. 100-104.

Gu, P., Shih, C. F., and Suo, Z., 1992, manuscript in preparation.

Huang, Y., and Hutchinson, J. W., 1989, "A Model Study of the Role of Nonuniform Defect Distribution on Plastic Shear Localization," *Role of Modeling in Materials Design*, ed. J. D. Embury, AIME.

Hutchinson, J. W., and Jensen, H. M., 1990, "Models of Fiber Debonding and Pullout in Brittle Composites with Friction," *Mech. Mater.* Vol. 9, pp. 139-163.

Marshall, D. B., Cox, B. N., and Evans, A. G., 1985, "The Mechanics of Matrix Cracking in Brittle Matrix Composites," *Acta Metall.*, Vol. 33, pp. 2013-2021.

Marshall, D. B., and Cox, B. N., 1987, "Tensile Fracture of Brittle Matrix Composites: Influence of Fiber Strength," *Acta Metall.*, Vol. 35, pp. 2607-2619.

Needleman, A., 1990, "An Analysis of Tensile Decohesion along an Interface," *J. Mech. Phys. Solids*, Vol. 38, pp. 289-324.

Peterson, R. E., 1974, *Stress Concentration Factors*, John Wiley, New York.

Rice, J. R., 1976, "The Localization of Plastic Deformation," *Proc. 14th IUTAM Congress*, pp. 207-220.

Rice, J. R., 1992, "Dislocation Nucleation from a Crack Tip: an Analysis based on the Peils Concept," *J. Mech. Phys. Solids*, Vol. 40, pp. 239-271.

Rose, L. R. F., 1987, "Crack Reinforcement by Distributed Springs," *J. Mech. Phys. Solids*, Vol 35, pp. 383-405.

Soutis, C., Fleck, N. A., and Smith, P. A., 1991, "Failure Prediction Technique for Compression Loaded Carbon Fiber-Epoxy Laminate with Open Hole," *J. Composite Materials*, Vol. 25, p. 1476.

Suo, Z., 1991, "Mechanics Concepts for Failure in Ferroelectric Ceramics," *Smart Structures and Materials*, ed., A. V. Srinivasan, ASME, New York, pp. 1-16.

Suo, Z., Bao, G., and Fan, B., 1992a, "Delamination R-Curve Phenomena due to Damage," *J. Mech. Phys. Solids*, Vol. 40, pp. 1-16.

Suo, Z., Ortiz, M., and Needleman, A., 1992b, "Stability of Solids with Interfaces," *J. Mech. Phys. Solids*, Vol. 40, pp. 613-640.

Tada, H., Paris, P. C., and Irwin, G. R., 1985, *The Stress Analysis of Cracks Handbook*, Del Research, St. Louis, MO.

Zok, F. W., and Spearing, S. M., 1992, "Matrix Crack Spacing in Brittle Matrix Composites," *Acta Met. Mater.*, Vol. 40, pp. 2033-2043.


## APPENDIX

Representative bridging laws are drawn in Fig. 2. Solutions for a hole/crack in an infinite body are reviewed here. For the *rectilinear law*, the solution is linear in both the applied stress and the closure-stress, so that

$$\delta_{tail} E'/a = f_1 \bar{\sigma} - f_2 \sigma_0, \quad (A1)$$

and

$$K_{tip}/\sqrt{a} = f_3 \bar{\sigma} - f_4 \sigma_0, \quad (A2)$$

with coefficients *fs* depending on $L/a$ only. For a crack-like notch the solution is (Tada et al. 1985)

$$\frac{\delta_{tail} E'}{\sigma_0 a} = 4(\eta^2 - 1)^{1/2} \left[ \frac{\bar{\sigma}}{\sigma_0} - \frac{2}{\pi} \cos^{-1}(1/\eta) \right] + \frac{8}{\pi} \ln \eta, \quad (A3)$$

and

$$\frac{K_{tip}}{\sigma_0 \sqrt{\pi a}} = \eta^{1/2} \left[ \frac{\bar{\sigma}}{\sigma_0} - \frac{2}{\pi} \cos^{-1}(1/\eta) \right], \quad (A4)$$

where $\eta = 1 + L/a$. Coefficients for a circular hole are obtained by using finite elements (Ho, 1992).

The *square-root law* is written

$$\sigma/\sigma_0 = (\delta/\delta_0)^{1/2} \tag{A5}$$

The solutions take the forms (e.g., Gu et al., 1992)

$$\sigma_{tail}/\alpha\sigma_0 = \Sigma(\bar{\sigma}/\alpha\sigma_0, L/a), \tag{A6}$$

with $\sigma_{tail}$ being connected to $\delta_{tail}$ by the bridging law, and

$$K_{tip}/\alpha\sigma_0\sqrt{a} = \kappa(\bar{\sigma}/\alpha\sigma_0, L/a). \tag{A7}$$

Solutions for a crack-like notch are given by Marshall and Cox (1987), Bao and McMeeking (1992), and Cui and Budiansky (1992). Solutions for elliptic holes are given by Gu et al. (1992).

The *linear law* is written

$$\sigma/\sigma_0 = \delta/\delta_0, \tag{A8}$$

The coupled spring-substrate is linear, so that

$$\sigma_{tail}/\bar{\sigma} = g_1(\alpha, L/a), \tag{A9}$$

and

$$K_{tip}/\bar{\sigma}\sqrt{\pi a} = g_2(\alpha, L/a). \tag{A10}$$

Solutions for a crack-like notch are given by Rose (1987), and for elliptical holes by Gu et al. (1992).

The *linear softening* is an idealization of the following situation. Some bridging mechansims, notably ductile reinforcement, attain the limiting stress at a very small stretch, and the stress then drops with a long tail. The initial rising portion may be conveniently lumped into $\Gamma_0$, leaving the post-limit tail idealized to be linear softening. The bridging law is thus

$$\sigma/\sigma_0 = 1 - \delta/\delta_0. \tag{A11}$$

The reward for such a simplification is that the limiting-stress, $\sigma_0$, can be treated as a residual stress, so that the coupled substrate-spring becomes linear, which can be solved by using commercial finite element codes (e.g., Suo et al., 1992a). The solution is still of form (A1) and (A2), but now the coefficients depend on both $\alpha$ and $L/a$.